

## ARTICLE

## OPEN



# Precipitation trend increases the contribution of dry reduced nitrogen deposition

Weihua Chen<sup>1,10</sup>, Shiguo Jia<sup>2,10</sup>, Xuemei Wang<sup>1</sup>✉, Min Shao<sup>1</sup>✉, Wenhui Liao<sup>3</sup>, Alex Guenther<sup>1</sup>, Chris Flechard<sup>1</sup>, Pengfei Yu<sup>1</sup>, Buqing Zhong<sup>6</sup>, Ming Chang<sup>1</sup>, Weiwen Wang<sup>1</sup>, Jingying Mao<sup>1</sup>, Xuejun Liu<sup>1</sup>, Guirui Yu<sup>8</sup> and Gregory Carmichael<sup>9</sup>

Given the leveling off in oxidized nitrogen emissions around the world, the atmospheric deposition of reduced nitrogen ( $\text{NH}_x = \text{NH}_3 + \text{NH}_4^+$ ) has become progressively critical, especially dry deposition, which presents great threats to plant growth. A combination of historical deposition data of measured wet  $\text{NH}_x$  and modeled dry  $\text{NH}_x$  in China suggests that dry  $\text{NH}_x$  deposition has been increasing substantially ( $4.50\% \text{ yr}^{-1}$ ,  $p < 0.05$ ) since 1980. Here, chemical transport model (WRF-EMEP) results indicate that variation in  $\text{NH}_3$  emissions is not a dominant factor resulting in the continually increasing trends of dry  $\text{NH}_x$  deposition, while climate change-induced trends in precipitation patterns with less frequent light rain and more frequent consecutive rain events (with  $\geq 2$  consecutive rainy days) contribute to the increase in dry  $\text{NH}_x$  deposition. This will continue to shift  $\text{NH}_x$  deposition from wet to dry form at a rate of 0.12 and  $0.23\% \text{ yr}^{-1}$  ( $p < 0.05$ ) for the period of 2030–2100 in China under the RCP4.5 and RCP8.5 scenarios, respectively. Further analysis for North America and Europe demonstrates results similar to China, with a consistent increase in the contribution of dry  $\text{NH}_x$  deposition driven by changing precipitation patterns from  $\sim 30\%$  to  $\sim 35\%$ . Our findings, therefore, uncover the change of precipitation patterns has an increasing influence on the shifting of  $\text{NH}_x$  deposition from wet to dry form in the Northern Hemisphere and highlight the need to shift from total  $\text{NH}_x$  deposition-based control strategies to more stringent  $\text{NH}_3$  emission controls targeting dry  $\text{NH}_x$  deposition in order to mitigate the potential negative ecological impacts.

*npj Climate and Atmospheric Science* (2023)6:62 ; <https://doi.org/10.1038/s41612-023-00390-7>

## INTRODUCTION

Nitrogen deposition, an important component of the global nitrogen cycle, has increased twofold over the past 100 years globally<sup>1</sup> and by 60% from 1980 to 2010 in China<sup>2</sup>, as a result of reactive nitrogen emissions associated with rapid expansion in agriculture and increased fossil fuel combustion<sup>3</sup>. These reactive nitrogen species include reduced ( $\text{NH}_x = \text{NH}_3 + \text{NH}_4^+$ ) and oxidized ( $\text{NO}_y = \text{NO}_x$  ( $\text{NO} + \text{NO}_2$ ) + its oxidation products) compounds. Given the continual reductions in  $\text{NO}_x$  emissions,  $\text{NH}_x$  deposition has become increasingly important, with its contribution currently reaching 60–85% of the total nitrogen deposition in the United States and Europe<sup>4–6</sup>. Enhanced  $\text{NH}_x$  deposition is favorable for crop production and plant growth in nitrogen-limited regions<sup>7</sup>, whereas excess  $\text{NH}_x$  deposition causes greater damage to nitrogen-sensitive ecosystems, including global biodiversity loss and eutrophication, compared with  $\text{NO}_x$  deposition<sup>8</sup>.

The removal of  $\text{NH}_x$  from the atmosphere can occur by dry or wet processes<sup>1,9,10</sup>. Wet deposition occurs mainly through scavenging by rainfall, sleet, fog, snow, and hail<sup>2,11</sup>, while dry deposition occurs by vertical turbulent transfer to the earth's surface<sup>8,9</sup>. Dry  $\text{NH}_x$  deposition (often dominated by gaseous  $\text{NH}_3$ ) is a continuous process that drives plant species composition change and reduces species cover and diversity much faster, and inflicts greater threats to plant growth compared to the same unit

of wet  $\text{NH}_x$  deposition<sup>12,13</sup>. Previous studies have characterized the spatiotemporal variation and ecological effects of  $\text{NH}_x$  deposition; however, the main focus of these studies has been on wet  $\text{NH}_x$  deposition because it is relatively easy to measure in existing networks<sup>2,11</sup>, whereas long-term and large-scale dry  $\text{NH}_x$  deposition has been less studied due to the technical difficulty in directly measuring and monitoring dry deposition. It has been reported that dry  $\text{NH}_x$  deposition has been a critical component of total  $\text{NH}_x$  deposition in recent years<sup>14,15</sup>. Based on a combination of historical measurement-based wet  $\text{NH}_x$  deposition and model-based dry  $\text{NH}_x$  deposition data, Yu et al.<sup>16</sup> suggested that there has been a shift in the relative contributions of wet and dry deposition to total  $\text{NH}_x$  deposition in China from 1980 to 2015; wet deposition previously dominated total  $\text{NH}_x$  deposition, but the modeled ratio of dry to wet  $\text{NH}_x$  deposition ( $R_{\text{NH}_x(\text{dry/wet})}$ ) gradually rose from 1980 to 2015, to the point where wet and dry deposition now have an approximately equal contribution to total  $\text{NH}_x$  deposition (Fig. 1). Thus, there is an urgent need to better understand why dry  $\text{NH}_x$  deposition and  $R_{\text{NH}_x(\text{dry/wet})}$  have increased in China during the past decades according to the modeled deposition, especially when  $\text{NH}_3$  emissions have remained stable since 2005<sup>16</sup>.

The major factors that control the variation of  $\text{NH}_x$  deposition include emissions, meteorology, and land cover<sup>9,17,18</sup>. Chemical transport models (CTMs) have been widely used to investigate the

<sup>1</sup>Guangdong-Hongkong-Macau Joint Laboratory of Collaborative Innovation for Environmental Quality, Institute for Environmental and Climate Research, Jinan University, Guangzhou 510632, PR China. <sup>2</sup>School of Atmospheric Sciences, Guangdong Province Key Laboratory for Climate Change and Natural Disaster Studies, Sun Yat-sen University, Guangzhou 510275, PR China. <sup>3</sup>Guangdong University of Finance, Guangzhou 510521, PR China. <sup>4</sup>Department of Earth System Science, University of California, Irvine, CA 92697, USA. <sup>5</sup>INRA, Agrocampus Ouest, UMR1069 Sol Agro-hydrosysteme Spatialisation, 35042 Rennes, France. <sup>6</sup>Key Laboratory of Vegetation Restoration and Management of Degraded Ecosystems, South China Botanical Garden, Chinese Academy of Sciences, Guangzhou 510650, PR China. <sup>7</sup>Key Laboratory of Plant-Soil Interactions of MOE, College of Resources and Environmental Sciences, China Agricultural University, Beijing 100083, PR China. <sup>8</sup>College of Resources and Environment, University of Chinese Academy of Sciences, Beijing 100049, PR China. <sup>9</sup>Department of Chemical and Biochemical Engineering, University of Iowa, Iowa City, IA 52242, USA. <sup>10</sup>These authors contributed equally: Weihua Chen, Shiguo Jia. ✉email: eciwxm@jnu.edu.cn; mshao@jnu.edu.cn

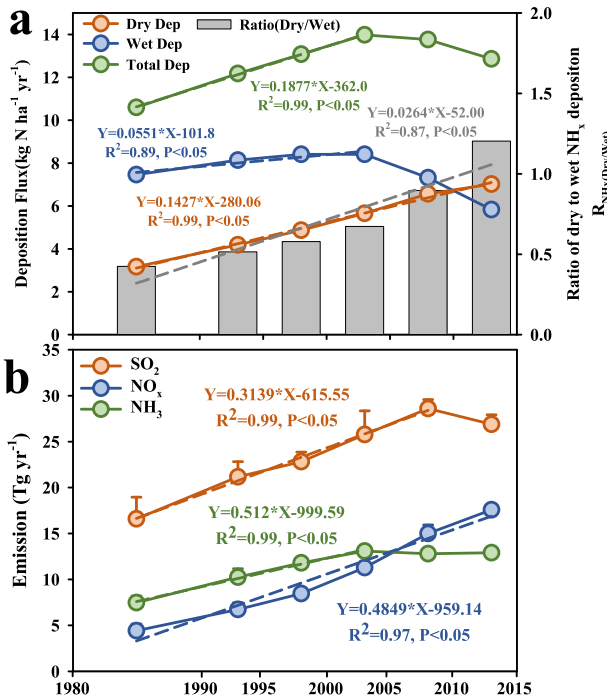


**Fig. 1 Temporal trends in NH<sub>x</sub> deposition and precursor emissions over China from 1980 to 2015.** **a**, Deposition flux (kg N ha<sup>-1</sup> yr<sup>-1</sup>) and the ratio of dry to wet NH<sub>x</sub> deposition ( $R_{\text{NHx}(\text{dry/wet})}$ ). **b**, Anthropogenic emissions of SO<sub>2</sub>, NO<sub>x</sub>, and NH<sub>3</sub> (Tg yr<sup>-1</sup>) (data obtained from Yu et al.<sup>16</sup>); circles represent the average modeled dry deposition, measured wet deposition, total deposition (dry + wet), and emissions for a given time period; the dashed lines are a linear fit to the points; gray bars are  $R_{\text{NHx}(\text{dry/wet})}$  and are plotted on the right-hand axis; error bars indicate standard deviation (s.d.).

relative impact of these factors on nitrogen deposition. The results suggest that the long-term trends of NH<sub>x</sub> deposition depend to a large extent on emissions and meteorology on regional and global scales, while land use and land cover are important for the spatial distribution of NH<sub>x</sub> deposition<sup>19–22</sup>. Specifically, variations in meteorological variables (e.g., precipitation, surface air temperature, wind speed, solar radiation, and atmospheric stability) driven by global climate change are closely related to the partitioning of dry and wet NH<sub>x</sub> deposition, although they play only a minor role (less than 20%) in controlling the long-term trends of total nitrogen deposition<sup>19–22</sup>. Precipitation, in particular, controls the partitioning of dry and wet NH<sub>x</sub> deposition due to its role in the wet scavenging process. Regardless of the importance of precipitation amount in the partitioning of dry and wet NH<sub>x</sub> deposition<sup>18,23</sup>, regional and global annual precipitation amounts have not shown a statistically significant trend in the past decades<sup>24</sup> and accordingly cannot explain the decadal-scale variation of the modeled partitioning of dry and wet NH<sub>x</sub> deposition. Precipitation patterns (e.g., occurrence, intensity, and duration), however, have changed significantly around the world. Specifically, extreme and consecutive rain events have intensified in the past 100 years<sup>25,26</sup> and are projected to intensify further in the future around the world<sup>27,28</sup>. The change in the precipitation patterns can be mainly attributed to the increased moisture in the atmosphere due to global warming and persistent low pressure due to the slowing of atmospheric circulation<sup>29,30</sup>. Nevertheless, the influence of changing precipitation patterns on the partitioning of dry and wet NH<sub>x</sub> deposition remains poorly understood<sup>19,20,23,31–33</sup>.

In this work, we address the following questions: how do the variations in climate change-induced precipitation patterns

contribute to the continual increase in dry NH<sub>x</sub> deposition and  $R_{\text{NHx}(\text{dry/wet})}$  in China<sup>15</sup>? Is the importance of climate change-induced precipitation patterns for the partitioning of dry and wet NH<sub>x</sub> deposition specific to China, or is it a ubiquitous phenomenon that also occurs in other regions worldwide? We first establish a linear emission-deposition response relationship based on CTM (WRF-EMEP) simulations to estimate the contribution of precursor emission variation to the change in dry NH<sub>x</sub> deposition and  $R_{\text{NHx}(\text{dry/wet})}$ . The change in dry NH<sub>x</sub> deposition and  $R_{\text{NHx}(\text{dry/wet})}$ , which cannot be explained by precursor emissions, suggests the effect of the interdecadal variability of precipitation patterns driven by climate change. We further explore the potential impact of future climate change on the partitioning of dry and wet NH<sub>x</sub> deposition by relying on prediction equations established through historical data and predicted data under two future climate change scenarios, representative concentration pathway (RCP) 4.5 and 8.5, for the period of 2030–2100. Finally, we broaden our analysis to include the United States (USA) and Europe, the other two hotspots of NH<sub>x</sub> deposition, to assess the universality of the increasing importance of dry NH<sub>x</sub> deposition. The purpose of this study is to advance our understanding of the partitioning of dry and wet NH<sub>x</sub> deposition driven by global climate change to date and in the future, which will have important implications for assessing ecological impacts and formulating policy to reduce NH<sub>3</sub> emissions in the face of climate change.

## RESULTS

### Historical perspective of NH<sub>x</sub> deposition

Historical NH<sub>x</sub> deposition data based on a combination of measured wet NH<sub>x</sub> deposition and modeled dry NH<sub>x</sub> deposition<sup>15</sup> (see “Methods” section for detailed information regarding data sources and methodology) for the period of 1980–2015 indicate that the total NH<sub>x</sub> deposition in China increased considerably at the rate of 0.188 kg N ha<sup>-1</sup> yr<sup>-2</sup> (1.77% yr<sup>-1</sup>,  $p < 0.05$ ) before 2005 and showed a slight decreasing trend (0.112 kg N ha<sup>-1</sup> yr<sup>-2</sup>, 0.80% yr<sup>-1</sup>) after 2005 (Fig. 1). On average, the total NH<sub>x</sub> deposition was estimated at  $12.7 \pm 1.1$  kg N ha<sup>-1</sup> yr<sup>-1</sup> in China from 1980 to 2015. In general, the variation in total NH<sub>x</sub> deposition was consistent and in line with the trends of NH<sub>3</sub> emissions, with a significant positive correlation observed between them ( $r = 0.95$ ,  $p < 0.05$ ).

With respect to the forms of NH<sub>x</sub> deposition, variation in wet NH<sub>x</sub> deposition was consistent with total NH<sub>x</sub> deposition, but the growth rate for wet NH<sub>x</sub> deposition (0.055 kg N ha<sup>-1</sup> yr<sup>-2</sup>, 0.74% yr<sup>-1</sup>) was lower than that of total NH<sub>x</sub> deposition before 2005, while the corresponding rate of decrease (0.258 kg N ha<sup>-1</sup> yr<sup>-2</sup>, 3.07% yr<sup>-1</sup>) was relatively higher after 2005. In contrast, modeled dry NH<sub>x</sub> deposition was on the rise during the study period, at the rate of 0.143 kg N ha<sup>-1</sup> yr<sup>-2</sup> (4.50% yr<sup>-1</sup>,  $p < 0.05$ ), leading to an upward trend for modeled  $R_{\text{NHx}(\text{dry/wet})}$  (ratio of dry to wet NH<sub>x</sub> deposition) at the rate of 0.026 per year (6.21% yr<sup>-1</sup>,  $p < 0.05$ ). These results indicate a shift in the relative contributions of wet and dry deposition to total NH<sub>x</sub> deposition, with modeled  $R_{\text{NHx}(\text{dry/wet})}$  increasing from 0.42 (1980s) to 1.20 (2010s), implying that China has gone from having wet deposition as the dominant contributor to total NH<sub>x</sub> deposition to having approximately equal dry and wet NH<sub>x</sub> deposition for the last two decades.

### Variation in deposition velocity is not responsible for the partitioning of NH<sub>x</sub> deposition

The dry deposition flux is calculated as the product of ambient concentration and vertical deposition velocity ( $V_d$ )<sup>5</sup> (see detailed information in Supplementary Note 1); ambient concentration depends heavily on precursor emissions while  $V_d$  relies heavily on meteorological conditions, surface characteristics, and the

pollution regime<sup>34–36</sup>. The parameterization of gaseous  $V_d$  utilizes a resistance approach analogous to Ohm's law in electrical circuits<sup>34–36</sup> (see detailed information in Supplementary Note 1). The resistance includes aerodynamic resistance ( $R_a$ ), quasi-laminar sublayer resistance ( $R_b$ ) and canopy resistance ( $R_c$ ), among which,  $R_c$  is generally the most dynamic and difficult to estimate<sup>37–40</sup>. Furthermore,  $R_c$  is dominant in the deposition process as it is typically the largest in magnitude among the three resistances<sup>40</sup>. Non-stomatal resistance ( $R_{ns}$ ) is one of the most important terms of  $R_c$  for gaseous  $\text{NH}_3$   $V_d$  since non-stomatal uptake is the dominant pathway for highly water-soluble gaseous  $\text{NH}_3$ <sup>37,38</sup>.  $R_{ns}$  is mostly influenced by surface temperature, relative humidity, and the presence of other trace substances (i.e.,  $\text{SO}_2$  and  $\text{NH}_3$ )<sup>38,39</sup>. According to the work of Simpson et al.<sup>39</sup>,  $R_{ns}$  was calculated in this study (see Supplementary Eqs. (3 and 4)). Stomatal resistance,  $R_{ns}$ , did not change significantly during the study period (Supplementary Fig. 1), although surface temperature (Supplementary Fig. 2) and precursor emissions (Fig. 1b) changed substantially in the past few decades. Further evidence provided by the WRF-EMEP model also revealed that the annual average  $V_d$  for gaseous  $\text{NH}_3$  and particulate  $\text{NH}_4^+$  had no obvious change between 2010 and 2017 (Supplementary Fig. 3, see detailed information in Supplementary Note 5). The results suggest that  $V_d$  affected by anthropogenic emissions and meteorology was not responsible for the partitioning of dry and wet  $\text{NH}_x$  deposition.

### Variation in emissions is not a dominant factor affecting the partitioning of $\text{NH}_x$ deposition

Among the precursor emissions,  $\text{NH}_3$  emissions are the primary driver determining the magnitude and trends of  $\text{NH}_x$  deposition. On the other hand, emissions of the acidic gases  $\text{SO}_2$  and  $\text{NO}_x$  can affect the equilibrium between gaseous  $\text{NH}_3$  and particulate  $\text{NH}_4^+$  through the variation of aerosol acidity. The variation in aerosol acidity can, in turn, influence the partitioning of dry and wet  $\text{NH}_x$  deposition<sup>11,14</sup>. In order to quantify the contribution of variations in precursor emissions to the change in modeled dry  $\text{NH}_x$  deposition and  $R_{\text{NH}x(\text{dry/wet})}$ , we first establish a linear emission-deposition response relationship based on CTM (WRF-EMEP) simulations (see "Methods" section for detailed information). As a result, we estimated that the changes in precursor emission amounts during 1985–2015, with values of +5.4 (+73%  $\text{yr}^{-1}$ ), +10.3 (+62%  $\text{yr}^{-1}$ ), and +13.2 (298%  $\text{yr}^{-1}$ )  $\text{Tg yr}^{-1}$  for  $\text{NH}_3$ ,  $\text{SO}_2$ , and  $\text{NO}_x$ , respectively, resulted in changes of +1.00  $\text{kg N ha}^{-1} \text{yr}^{-1}$  and +0.03 for the variation in modeled dry  $\text{NH}_x$  deposition ( $\Delta\text{Dry}$ ) and modeled  $R_{\text{NH}x(\text{dry/wet})}$  ( $\Delta\text{Ratio}$ ), respectively. To summarize, changes in precursor emissions explained 26% of the increase in modeled dry  $\text{NH}_x$  deposition and 4% of the increase in modeled  $R_{\text{NH}x(\text{dry/wet})}$ , with an overall variation of +3.85  $\text{kg N ha}^{-1} \text{yr}^{-1}$  and +0.78 for  $\Delta\text{Dry}$  and  $\Delta\text{Ratio}$ , respectively, suggesting that variation in anthropogenic emissions is not a dominant factor affecting the partition of dry and wet  $\text{NH}_x$  deposition from the perspective of long-term trends. This finding is also confirmed by the spatial analysis of  $\text{NH}_x$  deposition (Supplementary Fig. 4) and anthropogenic emissions (Supplementary Fig. 5), which corroborate the finding from the temporal analysis that variation in anthropogenic emission is not a dominant factor affecting the partition of dry and wet  $\text{NH}_x$  deposition (Supplementary Note 3).

### Effect of climate change-induced precipitation patterns on the partitioning of $\text{NH}_x$ deposition

It is widely accepted that precipitation amount is the most important meteorological factor affecting the magnitude of  $\text{NH}_x$  deposition flux<sup>18,41</sup>. However, there has been no significant variation in the long-term annual accumulated precipitation amount in China during the past few decades, with an average value of 1009–1047  $\text{mm yr}^{-1}$  (Supplementary Fig. 6a). In addition,

there has been no statistically significant correlation between precipitation amount and modeled dry  $\text{NH}_x$  deposition, modeled  $R_{\text{NH}x(\text{dry/wet})}$ , suggesting that interdecadal variability in precipitation amount is not sufficient to explain the upward trends in modeled dry  $\text{NH}_x$  deposition and  $R_{\text{NH}x(\text{dry/wet})}$ . However, precipitation patterns (e.g., intensity and duration) have changed significantly around the world despite stable precipitation amounts. In order to characterize rain intensity and rain event duration quantitatively, rain intensity was classified as light rain ( $0.1\text{--}10 \text{ mm d}^{-1}$ ) and moderate rain or above ( $\geq 10 \text{ mm d}^{-1}$ ). Based on rainfall duration, a rain event was classified as a consecutive rain event (with two or more consecutive rainy days) or a single rain event.

As shown in Supplementary Fig. 6b, c, the frequency of light rain decreased significantly while upward trends were observed for consecutive rain events in China during 1985–2015 under the effect of climate change. Moreover, the frequency of light rain was negatively correlated with modeled dry  $\text{NH}_x$  deposition ( $r = -0.73$ ) and modeled  $R_{\text{NH}x(\text{dry/wet})}$  ( $r = -0.90$ ), and the occurrence of consecutive rain events was positively correlated with modeled dry  $\text{NH}_x$  deposition ( $r = 0.55$ ) and modeled  $R_{\text{NH}x(\text{dry/wet})}$  ( $r = 0.70$ ), indicating that rain intensity and rain event duration may be responsible for the upward trends in modeled dry  $\text{NH}_x$  deposition and  $R_{\text{NH}x(\text{dry/wet})}$  in China.

Previous studies have revealed that owing to global climate change, variation in precipitation patterns plays a more important role than the amount of rain in the removal of air pollutants<sup>42,43</sup>. In terms of rain intensity, it has been theoretically and empirically proven that pollutant concentration in rainwater has a negative correlation with rainfall intensity and that light rain is the most effective at removing water-soluble pollutants through below-cloud scavenging processes<sup>44–49</sup>. Wang et al.<sup>50</sup> further demonstrated that aerosol wet scavenging on a global scale is predominantly constrained by light rain and that the magnitude of scavenging varies approximately exponentially with precipitation intensity. To verify the relationship between the wet removal of  $\text{NH}_4^+$  and rain intensity, the concentration of  $\text{NH}_4^+$  in rainfall and the rain intensity was analyzed with data across China, the USA, and Europe. Results showed an exponential relationship between the two parameters, with  $r$ -squared values above 0.80 and  $p$ -values less than 0.001 (Supplementary Fig. 7, see Supplementary Note 2.1 for data sources), providing additional evidence that light rain has a stronger washout capacity for  $\text{NH}_4^+$  globally. With respect to rain event duration, the washout amount of  $\text{NH}_4^+$  from the atmosphere by consecutive rain events is less than that by an equivalent amount of inconsecutive rain events. This is because as a rain event continues, less  $\text{NH}_x$  content is removed from the atmosphere due to less available  $\text{NH}_3$  in the atmosphere.  $\text{NH}_3$  is less available because of suppressed  $\text{NH}_3$  emissions during the rainfall process and less accumulated  $\text{NH}_3$  due to washout in the previous time period<sup>51</sup>. As an example, the dynamics of  $\text{NH}_4^+$  concentrations recorded during two consecutive rain events on April 11th, 2009, in Guiyang, China, revealed that  $\text{NH}_4^+$  was scavenged quickly at the start of each precipitation event, followed by a relatively low level of scavenging until the end of the event<sup>41</sup> (Supplementary Fig. 8).

In order to characterize the precipitation pattern-induced effect on the below-cloud wet removal of  $\text{NH}_x$  content with the co-influence of rain intensity and rain event duration, we have defined a new indicator, the precipitation scavenging index (PSI), in this study. The PSI is calculated as follows:

$$\text{PSI} = \frac{\text{LR}}{\text{CR}} \quad (1)$$

Where LR represents the frequency of days with light rain each year, and CR represents the occurrence of consecutive rain events each year. PSI is, therefore, a dimensionless indicator. A lower value of PSI suggests that less frequent but increasingly intense

rainfall events are less efficient at "cleaning" the atmosphere of gaseous  $\text{NH}_3$  and particulate  $\text{NH}_4^+$ . This implies that more  $\text{NH}_x$  remains in the atmosphere for dry deposition by turbulent diffusion to vegetation and other surfaces. This indicator, despite not having a specific physical meaning, provides a simple way to reflect the negative correlation between LR and dry  $\text{NH}_x$  deposition and  $R_{\text{NHx(dry/wet)}}$ , as well as the positive correlation between CR and dry  $\text{NH}_x$  deposition and  $R_{\text{NHx(dry/wet)}}$ , and comprehensively represents the contrasting effect of LR and CR on the below-cloud wet removal of  $\text{NH}_x$ .

An overall negative trend was found for PSI in China during 1980–2015 (Fig. 2). The negative correlations were found between PSI and modeled dry  $\text{NH}_x$  deposition ( $r = -0.79$ ) as well as modeled  $R_{\text{NHx(dry/wet)}}$  ( $r = -0.63$ ), indicating that variation in climate change-induced precipitation patterns favor a shift in  $\text{NH}_x$  deposition from the wet to dry form. Spatial analysis of  $\text{NH}_x$  deposition (Supplementary Fig. 4) and precipitation patterns (Supplementary Fig. 9) in China further confirmed that changing precipitation patterns contributed to the increase in dry  $\text{NH}_x$  deposition in China (Supplementary Note 3). Our finding is supported by studies conducted in the USA, which also revealed that most of the increases in ambient  $\text{NH}_3$  concentration are a manifestation of climate change<sup>52,53</sup>.

### Implications for future partitioning of $\text{NH}_x$ deposition

As global climate change is accelerating, partitioning of dry and wet  $\text{NH}_x$  deposition driven by precipitation pattern changes is expected to continue in the future. The results from the two future global climate scenarios (RCP4.5 and RCP8.5) show that less frequent light rain and more consecutive rain events are expected for the period of 2030–2100 (Supplementary Fig. 6b, c). Therefore, the PSI will continue to decline in the future (Fig. 2), implying that more  $\text{NH}_x$  remains in the atmosphere and can subsequently be removed from the atmosphere via dry deposition processes. Further reductions in anthropogenic  $\text{SO}_2$  and  $\text{NO}_x$  emissions, and a steady increase in  $\text{NH}_3$  emissions, are projected from 2030 to 2100 under these global climate scenarios (Supplementary Fig. 10). Hence, the projected  $R_{\text{NHx(dry/wet)}}$ , as a function of the emission index (EI) and PSI (see detailed information in Supplementary Note 6), will continue to increase between 2030 and 2100 at a rate of 0.007 per year ( $0.59\% \text{ yr}^{-1}$ ,  $p < 0.05$ ) and 0.010 per year ( $1.13\% \text{ yr}^{-1}$ ,  $p < 0.05$ ) for the RCP4.5 and RCP8.5 scenarios, respectively (Fig. 3a). As a result, modeled dry  $\text{NH}_x$  deposition shows increasing trends at a rate of  $0.011 \text{ kg N ha}^{-1} \text{ yr}^{-2}$  ( $0.16\% \text{ yr}^{-1}$ ,  $p < 0.05$ ) for RCP4.5 and  $0.020 \text{ kg N ha}^{-1} \text{ yr}^{-2}$  ( $0.30\% \text{ yr}^{-1}$ ,  $p < 0.05$ ) for RCP8.5, respectively (Fig. 3b). Accordingly, based on the projected dry  $\text{NH}_x$  deposition and  $R_{\text{NHx(dry/wet)}}$ ,

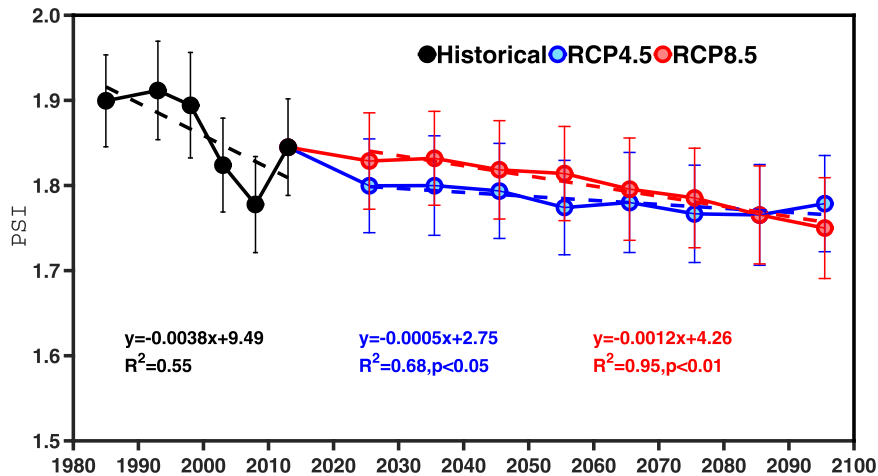


**Fig. 2 Long-term trends of the historical (1980–2015) and predicted (2030–2100) precipitation scavenging index (PSI) in China.** Predicted PSI was calculated by using the meteorological parameters from the two global future climate change scenarios RCP 4.5 and RCP 8.5. Error bars indicate 1/3 standard deviation (s.d.).

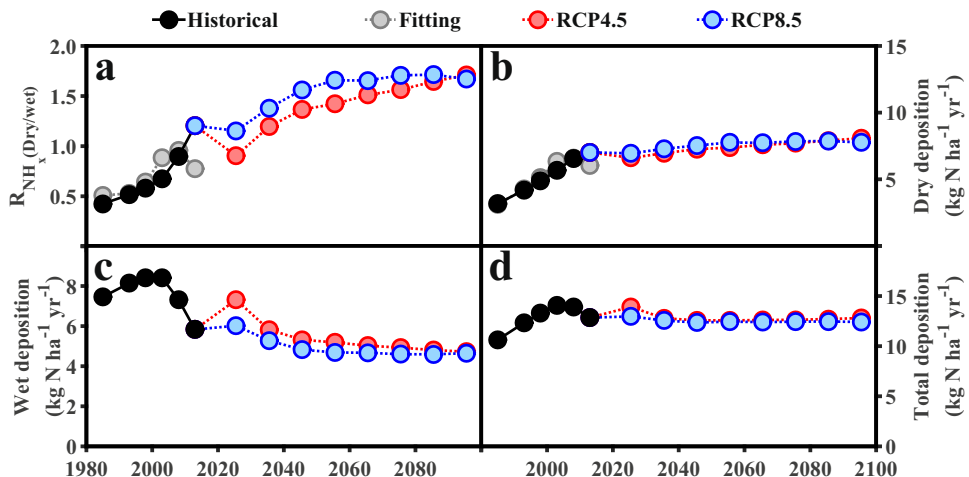


**Fig. 3 Temporal variations of  $\text{NH}_x$  deposition and  $R_{\text{NHx(dry/wet)}}$  in China over the historical (1980–2015) and future period (2030–2100).** **a**  $R_{\text{NHx(dry/wet)}}$ ; **b** dry deposition; **c** wet deposition; **d** total deposition.

we extrapolated that wet  $\text{NH}_x$  deposition shows a continuing downward trend (Fig. 3c), while the total  $\text{NH}_x$  deposition remains stable since  $\text{NH}_3$  emissions remain constant (Fig. 3d). Even though the total  $\text{NH}_x$  deposition remains almost stable at around 12–13 kg  $\text{N ha}^{-1} \text{yr}^{-1}$  in the future, the threats to natural ecosystems from  $\text{NH}_x$  deposition are expected to increase in the future since the projected increase in dry  $\text{NH}_x$  deposition could lead to greater damage to plant growth as compared to a similar amount of wet  $\text{NH}_x$  deposition<sup>12,13</sup>. Meanwhile, the shifting of the partitioning of  $\text{NH}_x$  deposition will also affect the air quality<sup>16,54,55</sup>. This is because the shifting of the partitioning of  $\text{NH}_x$  deposition from the particulate phase to the gaseous phase would decrease particle pollution to some extent<sup>54</sup>. However, the shifting of the partitioning of  $\text{NH}_x$  deposition would increase the lifetime of  $\text{NH}_x$ , and this can facilitate long-range transportation of  $\text{NH}_x$ , which may affect other regions<sup>55</sup>.

## DISCUSSION

In light of the importance of dry  $\text{NH}_x$  deposition to the nitrogen cycle and the associated ecological effects, we broaden our analysis to historical  $\text{NH}_x$  deposition data in the USA and Europe, which are recognized as additional hotspots of  $\text{NH}_x$  deposition (see more details in Supplementary Note 2.1 and Supplementary Note 4). Consistent upward trends for modeled  $R_{\text{NH}_x(\text{dry/wet})}$  also

occur in the USA and Europe, irrespective of changes in total, wet, and dry deposition of  $\text{NH}_x$  (Supplementary Fig. 11). Specifically, modeled  $R_{\text{NH}_x(\text{dry/wet})}$  increased at a rate of 0.010 per year ( $2.05\% \text{ yr}^{-1}$ ,  $p < 0.05$ ) in the USA and 0.005 per year ( $1.19\% \text{ yr}^{-1}$ ,  $p < 0.05$ ) in Europe. Although wet deposition remained the dominant mechanism for  $\text{NH}_x$  removal in the USA and Europe, the contribution of modeled dry  $\text{NH}_x$  deposition to total  $\text{NH}_x$  deposition increased in the past two decades, from ~30% to ~35% for both the USA and Europe. Similar to the estimation in China, we extrapolate that precipitation pattern variations driven by climate change offset the effect of stable or decreasing  $\text{NH}_3$  emissions and increase the contribution of modeled dry  $\text{NH}_x$  deposition to total  $\text{NH}_x$  deposition in the USA and Europe (see detailed information in Supplementary Note 4).

The results from the two additional continents further suggest the widespread and growing importance of dry  $\text{NH}_x$  deposition driven by precipitation patterns resulting from global climate change. This is in contrast with previous studies that suggest relatively little influence of climate change, which may partly be because they only considered changes in precipitation amount, whereas we show that precipitation patterns (intensity and duration) play a far more important role in the shifting of  $\text{NH}_x$  deposition partitioning<sup>19–22</sup>. Figure 4 schematically illustrates how  $\text{NH}_x$  deposition partitioning shifts under the influence of climate change-induced variations in precipitation patterns. In view of the

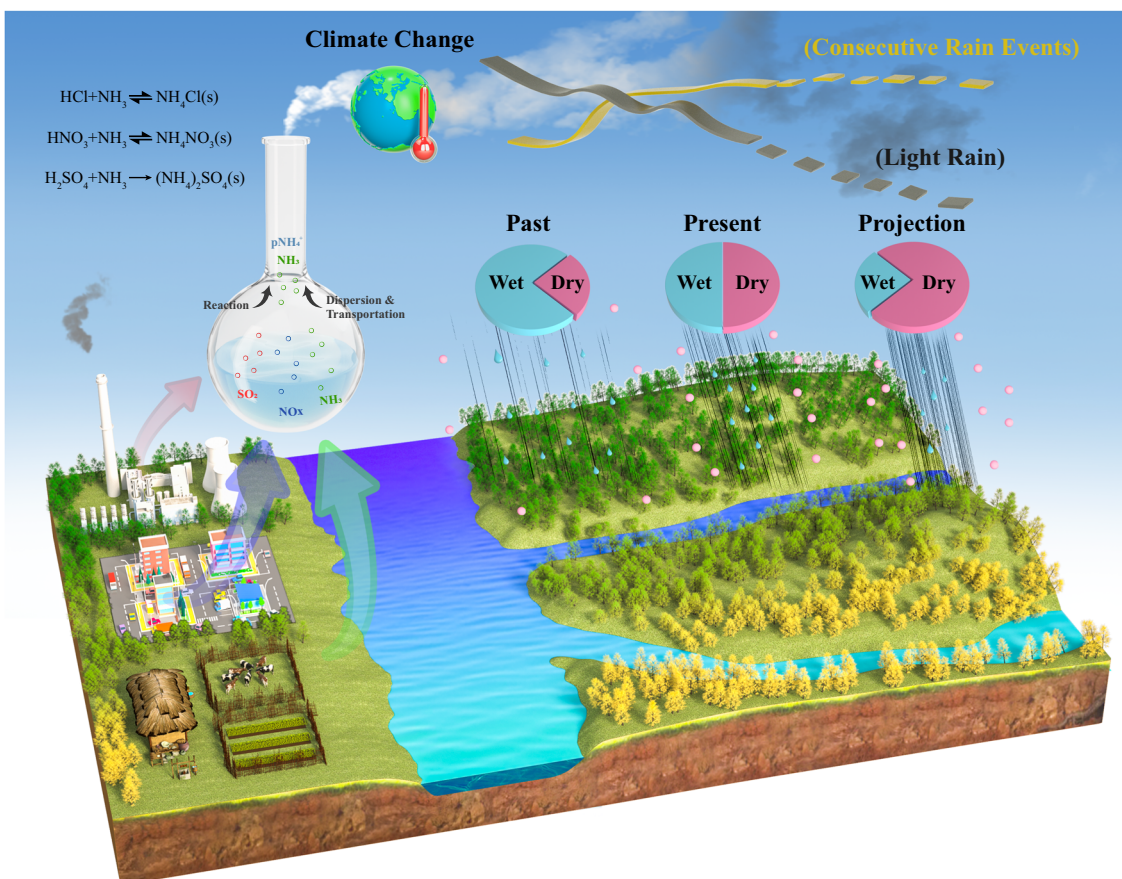


**Fig. 4 Schematic representation of the shift in  $\text{NH}_x$  deposition partitioning driven by climate change-induced variations in precipitation patterns.** Atmospheric reduced nitrogen ( $\text{NH}_x$ ) is emitted in the form of  $\text{NH}_3$  to a large extent by agricultural activities (nitrogen fertilizer application and livestock manure) and then deposited back to the earth's surface via dry and wet removal pathways.  $\text{NH}_3$  emissions, in combination with emissions of the acidic gases  $\text{SO}_2$  and  $\text{NO}_x$ , can influence the partitioning of dry and wet  $\text{NH}_x$  deposition by affecting the equilibrium between gaseous  $\text{NH}_3$  and particulate  $\text{NH}_4^+$ <sup>11,18</sup>. More importantly, as a consequence of climate change, global trends in precipitation patterns, in particular trends toward less frequent light rain and more frequent consecutive rain events, shift the partitioning of the dry and wet deposited  $\text{NH}_x$  fractions. Specifically, this leads to a decrease in wet deposition and an increase in dry deposition, leading to negative ecological consequences since the continued increasing dry  $\text{NH}_x$  deposition causes greater damage to plant growth as compared to the same unit of wet  $\text{NH}_x$  deposition<sup>12,13</sup>.

acceleration of global climate change, less frequent light rain and more frequent consecutive rain events are expected at present and in the coming decades. In particular, extreme rain events are projected to become more frequent in the future, which will further strengthen the shifting of  $\text{NH}_x$  deposition from the wet to the dry form. Consequently, relatively less  $\text{NH}_x$  content will be removed from the atmosphere via wet deposition, resulting in a continued increase in the contribution of dry  $\text{NH}_x$  deposition, which will have a series of side effects on natural ecosystems and human health and air quality<sup>12,54,56</sup>. More importantly, other extreme weather events (e.g., drought and heatwave) due to global climate change will weaken the growth of plants and increase their susceptibility to increased dry  $\text{NH}_x$  deposition in the future<sup>57</sup>.

Note that changes in  $\text{NH}_x$  deposition can reflect the tendency of total nitrogen deposition to a certain extent, although we focus only on the partitioning of dry and wet  $\text{NH}_x$  deposition in this study without analyzing  $\text{NO}_y$  deposition. For example, the increasing importance of  $\text{NH}_x$  deposition compared with  $\text{NO}_y$  deposition can be inferred based on the combination of historically measured wet nitrogen deposition and modeled dry nitrogen deposition data shown in Yu et al.<sup>16</sup>. Looking to the future,  $\text{NH}_x$  deposition will dominate total nitrogen deposition after 2030, as  $\text{NH}_3$  emissions are expected to surpass  $\text{NO}_x$  emissions at that time (Supplementary Fig. 10), suggesting that the role of  $\text{NH}_x$  deposition in nitrogen deposition will become more prominent, especially with the continued strict control of  $\text{NO}_x$  emissions. Lamarque et al.<sup>58</sup> also reported that nitrogen deposition was projected to increase over certain regions around the world by the end of the 21st century, especially in Asia, owing to the projected increase in  $\text{NH}_3$  emissions. Consequently,  $\text{NH}_3$  emission control is still the most effective and fundamental way to reduce  $\text{NH}_x$  deposition and to curb its damage to natural ecosystems and human health, although  $\text{NH}_3$  emission abatement cannot fully control  $\text{NH}_x$  deposition as previous studies documented that per-unit reduction in  $\text{NH}_3$  emissions led to only a 60–80% mitigation of  $\text{NH}_x$  deposition<sup>10,59</sup>. Nevertheless, the analysis in the USA and Europe also highlights that the expected benefits from  $\text{NH}_3$  emission reductions on dry  $\text{NH}_x$  deposition are diminished by the effects of climate change. Hence, more stringent  $\text{NH}_3$  emission controls are required to achieve the desired reductions in  $\text{NH}_x$  deposition levels in the future<sup>20</sup>. A significant proportion of the  $\text{NH}_3$  emissions in China can be attributed to its agricultural sources, and improving agricultural nitrogen management (e.g., reduced fertilizer application, covered manure storage, and implementation of the deep application of fertilizers during growing seasons) could be the most effective approach to reduce  $\text{NH}_3$  emissions from agricultural sources in China to date and in the future<sup>54,60,61</sup>.

This study prompts our re-examination of the significance of dry  $\text{NH}_x$  deposition in the global nitrogen cycle and ecosystem assessment and poses an urgent need to mitigate  $\text{NH}_x$  deposition in the face of global climate change. Nevertheless, this study is still subject to four major uncertainties and limitations (see more information in Supplementary Note 7): (1) Long-term trends of dry  $\text{NH}_x$  deposition are modeled results, which entail a higher degree of uncertainty than the observed wet  $\text{NH}_x$  deposition<sup>11,62,63</sup>. Deposition velocity ( $V_d$ ) is the dominant contributor to the uncertainty of dry deposition simulations and could potentially affect the estimation of dry  $\text{NH}_x$  deposition flux<sup>34–36</sup>. However, year-specific instead of time-varying  $V_d$  was used to estimate long-term trends of dry  $\text{NH}_x$  deposition in this study, which could introduce additional uncertainties. (2) The historical  $\text{NH}_3$  emissions data were calculated based on bottom-up activity data and static emissions factors, which did not consider the effect of interannual meteorological variability<sup>64–67</sup>. Whereas  $\text{NH}_3$  emissions were extremely weather/climate-sensitive<sup>68</sup>, the influence of climate change-induced precipitation patterns and other meteorological

factors (e.g., temperature and wind speed) are supposed to affect the emission processes of  $\text{NH}_3$ , which might also introduce additional uncertainties. (3) The land/atmosphere exchange of gaseous  $\text{NH}_3$  is, in fact, bi-directional and controlled by a range of environmental factors<sup>69–71</sup>. Nonetheless, owing to the difficulty of obtaining detailed input parameters and empirical tuning at a large scale,  $\text{NH}_3$  bi-directional exchange process has been incorporated into only a few of the regional- and global-scale CTMs (i.e., CMAQ, CAM<sub>x</sub>, GEM-MACH, and LOTOS-EUROS)<sup>35,36,72,73</sup>. Therefore, the lack of consideration of bi-directional parameterization schemes simultaneously affects the estimation of  $\text{NH}_3$  emissions and  $\text{NH}_x$  deposition<sup>74–76</sup> and introduces additional uncertainties. (4) Apart from precipitation patterns, global climate change can also affect  $\text{NH}_x$  deposition partitioning through other aspects such as surface temperature, solar radiation, relative humidity, soil temperature, and natural surface properties<sup>68,77,78</sup>. However, the complex interactions of multiple meteorological parameters, as opposed to their individual effects on  $\text{NH}_x$  deposition partitioning, make it difficult to isolate and quantify the relative importance of these meteorological parameters. Hence, the quantification of global climate change-induced  $\text{NH}_x$  deposition partitioning is still subject to large uncertainty and remains a great challenge for the whole community. Development of climate-dependent models for better quantification of the dynamic relationship between  $\text{NH}_3$  emissions, climate/meteorology, and deposition under global environmental change in the future is therefore needed<sup>77</sup>.

## METHODS

### Historical dry and wet $\text{NH}_x$ deposition data in China

Both the annual modeled dry  $\text{NH}_x$  deposition and measured wet  $\text{NH}_x$  deposition data in China for the period of 1980–2015 were obtained from Yu et al.<sup>16</sup>, which is the most comprehensive and current data on long-term  $\text{NH}_x$  deposition available in China. General information regarding the sources of the  $\text{NH}_x$  deposition data collected in China has been summarized in Supplementary Table 1. Briefly, observed wet  $\text{NH}_x$  deposition data were obtained from four sources, including (1) peer-reviewed published papers screened by Yu et al.<sup>16</sup>, (2) the Acid Deposition Monitoring Network in East Asia (<https://www.eanet.asia/>, last access: 3 January 2023), (3) the National Ecosystem Research Network of China (<http://www.cnern.ac.cn/index.action>, last access: 3 January 2023), and (4) the Nationwide Nitrogen Deposition Monitoring Network established by China Agricultural University<sup>72</sup>, with a total of 956 monitoring sites.

Modeled dry  $\text{NH}_x$  deposition fluxes were obtained from inferential methods, which combine ambient concentrations and dry deposition velocities (see Supplementary Note 1 for the parameterization of dry  $\text{NH}_3$  deposition)<sup>5,79,80</sup>. The average land use specific  $V_d$  collected from previous studies was used to calculate annual dry  $\text{NH}_x$  deposition (Supplementary Fig. 12, see Extended Data Table 4 in Yu et al.<sup>16</sup>). Specifically, modeled  $V_d$  for 9 land use types was derived from Xu et al.<sup>11</sup>, who applied the GEOS-Chem model coupled with the scheme of Wesely<sup>81</sup> and Zhang et al.<sup>82</sup> to calculate  $V_d$  for gaseous  $\text{NH}_3$  and particulate  $\text{NH}_4^+$ , respectively. Modeled  $V_d$  in the rest of 5 land use types (i.e., desert, tundra, water, wetland, and ice) was estimated by using similar parameterization schemes used as in Xu et al.<sup>11</sup> but with different CTMs (CMAQ, RegAMDS)<sup>83–88</sup>. It is worth noting that the modeled  $V_d$  in the 14 land use types derived from Yu et al.<sup>16</sup> was originally based on a unidirectional method, except for Su et al.<sup>83</sup>, who used a bi-directional  $\text{NH}_3$  exchange method to calculate  $V_d$  for gaseous  $\text{NH}_3$  over deserts.

Yu et al.<sup>16</sup> averaged the annual  $\text{NH}_x$  deposition during 1980–2015 for 6 periods, including 1980–1990, 1991–1995, 1996–2000, 2001–2005, 2006–2010, and 2011–2015<sup>15</sup>. Hence, we

also averaged precursor emissions for the corresponding six periods (see Supplementary Note 2.3 for detailed information regarding emissions data). The data in each period were fitted with the middle year of the corresponding period in order to obtain the linear regressions. Subsequently, the slope of the linear regression was used to represent the average annual rate of change. The relative annual rate of change was then calculated by normalizing the annual rate of change with the value for the first time period in each region.

### Quantification of the contribution of emissions to $\text{NH}_x$ deposition partitioning

The response relationship between  $\text{NH}_x$  deposition and precursor emissions was developed based on the WRF-EMEP model (the Weather Research and Forecasting model coupled with the European Monitoring and Evaluation Program)<sup>32</sup>. Model configuration and evaluation are presented in Supplementary Note 5. A series of sensitivity studies were conducted to quantify the response of  $\text{NH}_x$  deposition to reductions in  $\text{SO}_2$ ,  $\text{NO}_x$ , and  $\text{NH}_3$  separately, as well as  $\text{SO}_2 + \text{NO}_x + \text{NH}_3$  together. The reduction values for individual emissions were set to be 10%, 30%, 50%, 70%, and 90%, respectively. Sensitivity results show that the response of regional  $\text{NH}_x$  deposition to individual emission reductions is nearly linear. This is consistent with the study by Civerolo et al.<sup>19</sup>, which also revealed that the response of global nitrogen deposition to emissions was nearly linear based on six different tropospheric chemistry models. Furthermore, sensitivity results also revealed that the effect of  $\text{NH}_3$  emission variation is far more important than that of  $\text{SO}_2$  and  $\text{NO}_x$  emissions, which has also been found by previous studies<sup>74,89</sup>. Last but not least, the response to the co-reduction of  $\text{SO}_2 + \text{NO}_x + \text{NH}_3$  was nearly equal to the sum of the individual reductions of  $\text{SO}_2$ ,  $\text{NO}_x$ , and  $\text{NH}_3$ . Therefore, the total variations in dry  $\text{NH}_x$  deposition ( $\Delta\text{Dry}$ ) and  $R_{\text{NH}_x(\text{dry/wet})}$  ( $\Delta\text{Ratio}$ ) caused by precursor emissions during 1980–2015 can be obtained using Eq. (2):

$$\Delta\text{Dry or } \Delta\text{Ratio} = a_1 \times \Delta\text{SO}_2 + a_2 \times \Delta\text{NO}_x + a_3 \times \Delta\text{NH}_3 \quad (2)$$

Where  $a_1$ ,  $a_2$ , and  $a_3$  are constants, indicating the variations in dry  $\text{NH}_x$  deposition and  $R_{\text{NH}_x(\text{dry/wet})}$  caused by per-unit reduction in  $\text{SO}_2$ ,  $\text{NO}_x$ , and  $\text{NH}_3$  emissions, respectively, as listed in Supplementary Table 2.  $\Delta\text{SO}_2$ ,  $\Delta\text{NO}_x$ , and  $\Delta\text{NH}_3$  are the changes in  $\text{SO}_2$ ,  $\text{NO}_x$ , and  $\text{NH}_3$  emissions between 1980 and 2015, respectively.

### DATA AVAILABILITY

All data used in this study are available in the main text or the supplemental materials. Links to download the  $\text{NH}_x$  data (i.e., ambient concentration, precipitation concentration, and deposition flux) can be found in Supplementary Table 1. Links to download historical and predicted anthropogenic emissions data and meteorological data are provided in the Supplementary Note 2.

### CODE AVAILABILITY

We performed simulations using WRF v3.9.1 coupled with the EMEP rv4.17 model, which are freely available at <https://www2.mmm.ucar.edu/wrf/users/> (last access: 3 January 2023) and <https://github.com/metno/emep-ctm> (last access: 3 January 2023), respectively.

Received: 6 July 2022; Accepted: 25 May 2023;

Published online: 07 June 2023

### REFERENCES

- Galloway, J. N. et al. Nitrogen cycles: past, present, and future. *Biogeochemistry* **70**, 153–226 (2004).
- Liu, X. J. et al. Enhanced nitrogen deposition over China. *Nature* **494**, 459–462 (2013).
- Galloway, J. N. et al. Transformation of the nitrogen cycle: Recent trends, questions, and potential solutions. *Science* **320**, 889–892 (2008).
- Jiang, Z. et al. Unexpected slowdown of US pollutant emission reduction in the past decade. *Proc. Natl Acad. Sci. USA* **115**, 5099–5104 (2018).
- Li, Y. et al. Increasing importance of deposition of reduced nitrogen in the United States. *Proc. Natl Acad. Sci. USA* **113**, 5874–5879 (2016).
- Tomlinson, S. J., Carnell, E. J., Dore, A. J. & Dragosits, U. Nitrogen deposition in the UK at 1 km resolution from 1990 to 2017. *Earth Syst. Sci. Data* **13**, 4677–4692 (2021).
- Thomas, R. Q., Canham, C., Weathers, K. C. & Goodale, C. L. Increased tree carbon storage in response to nitrogen deposition in the US. *Nat. Geosci.* **3**, 13–17 (2010).
- Erisman, J. W. et al. Consequences of human modification of the global nitrogen cycle. *Philos. T. R. Soc. B* **368**, 20130116 (2013).
- Lamarque, J. F. et al. Assessing future nitrogen deposition and carbon cycle feedback using a multimodel approach: analysis of nitrogen deposition. *J. Geophys. Res.* **110**, D19303 (2005).
- Tan, J., Fu, J. S. & Seinfeld, J. H. Ammonia emission abatement does not fully control reduced forms of nitrogen deposition. *Proc. Natl Acad. Sci. USA* **117**, 9771–9775 (2020).
- Xu, W. et al. Quantifying atmospheric nitrogen deposition through a nationwide monitoring network across China. *Atmos. Chem. Phys.* **15**, 12345–12360 (2015).
- Sheppard, L. J. et al. Dry deposition of ammonia gas drives species change faster than wet deposition of ammonium ions: evidence from a long-term field manipulation. *Glob. Change Biol.* **17**, 3589–3607 (2011).
- Van der Erden, L. J. M. Toxicity of ammonia to plants. *Agric. Environ.* **7**, 223–235 (1982).
- Pan, Y. P. et al. Ammonia should be considered in field experiments mimicking nitrogen deposition. *Atmos. Ocean. Sci. Lett.* **13**, 248–251 (2020).
- Jia, Y. et al. Spatial and decadal variations in inorganic nitrogen wet deposition in China induced by human activity. *Sci. Rep.* **4**, 3763 (2014).
- Yu, G. et al. Stabilization of atmospheric nitrogen deposition in China over the past decade. *Nat. Geosci.* **12**, 424–429 (2019).
- Hertel, O. et al. Governing processes for reactive nitrogen compounds in the European atmosphere. *Biogeosciences* **9**, 4921–4954 (2012).
- Pan, Y. P. et al. Wet and dry deposition of atmospheric nitrogen at ten sites in Northern China. *Atmos. Chem. Phys.* **12**, 6515–6535 (2012).
- Civerolo, K. L. et al. Simted effects of climate change on summertime nitrogen deposition in the eastern US. *Atmos. Environ.* **42**, 2074–2082 (2008).
- Ellis, R. A. et al. Present and future nitrogen deposition to national parks in the United States: critical load exceedances. *Atmos. Chem. Phys.* **13**, 9083–9095 (2013).
- Zhang, J. et al. Impacts of cli change and emissions on atmospheric oxidized nitrogen deposition over East Asia. *Atmos. Chem. Phys.* **19**, 887–900 (2019).
- Zhao, X. et al. Spatial and temporal variation of inorganic nitrogen wet deposition to the Yangtze River Delta region, China. *Water Air Soil Pollut.* **203**, 277–289 (2009).
- Sun, Q. et al. A review of global precipitation data sets: data sources, estimation, and intercomparisons. *Rev. Geophys.* **56**, 79–107 (2018).
- Fischer, E. M. & Knutti, R. Observed heavy precipitation increase confirms theory and early models. *Nat. Clim. Change* **6**, 986–991 (2016).
- O'Gorman, P. A. Sensitivity of tropical precipitation extremes to climate change. *Nat. Geosci.* **5**, 697–700 (2012).
- Palmer, T. N. & Räisänen, J. Quantifying the risk of extreme seasonal precipitation events in a changing climate. *Nature* **415**, 512–514 (2002).
- Donat, M. G., Lowry, A. L., Alexander, L. V., O'Gorman, P. A. & Maher, N. More extreme precipitation in the world's dry and wet regions. *Nat. Clim. Change* **6**, 508–513 (2016).
- Butler, T., Vermeylen, F., Lehmann, C. M., Likens, G. E. & Puchalski, M. Increasing ammonia concentration trends in large regions of the USA derived from the NADP/AMON network. *Atmos. Environ.* **146**, 132–140 (2016).
- Kendon, E. J. Why extreme rains are gaining strength as the climate warms. *Nature* **563**, 461–461 (2018).
- Westra, W. et al. Future changes to the intensity and frequency of short-duration extreme rainfall. *Rev. Geophys.* **52**, 522–555 (2014).
- Langner, J., Bergström, R. & Foltescu, V. Impact of climate change on surface ozone and deposition of sulphur and nitrogen in Europe. *Atmos. Environ.* **39**, 1129–1141 (2005).
- Simpson, D. et al. Impacts of climate and emission changes on nitrogen deposition in Europe: a multi-model study. *Atmos. Chem. Phys.* **14**, 6995–7017 (2014).
- Kang, Y. et al. High-resolution ammonia emissions inventories in China from 1980 to 2012. *Atmos. Chem. Phys.* **16**, 2043–2058 (2016).
- Bash, J. O., Cooter, E. J., Dennis, R. L., Walker, J. T. & Pleim, J. E. Evaluation of a regional air-quality model with bidirectional  $\text{NH}_3$  exchange coupled to an agroecosystem model. *Biogeosciences* **10**, 1635–1645 (2013).

35. Sutton, M. A., Schjoerring, J. K. & Wyers, G. P. Plant-atmosphere exchange of ammonia. *Philos. Trans. R. Soc. A* **351**, 261–278 (1995).
36. Nair, A. A. & Yu, F. Quantification of atmospheric ammonia concentrations: a review of its measurement and modeling. *Atmosphere* **11**, 1092 (2020).
37. Flechard, C. R. et al. Dry deposition of reactive nitrogen to European ecosystems: a comparison of inferential models across the NitroEurope network. *Atmos. Chem. Phys.* **11**, 2703–2728 (2011).
38. Tanner, E., Buchmann, N. & Eugster, W. Agricultural ammonia dry deposition and total nitrogen deposition to a Swiss mire. *Agric. Ecosyst. Environ.* **336**, 108009 (2022).
39. Simpson, D. et al. The EMEP MSC-W chemical transport model—technical description. *Atmos. Chem. Phys.* **12**, 7825–7865 (2012).
40. Wu, Z. Y. et al. Evaluating the calculated dry deposition velocities of reactive nitrogen oxides and ozone from two community models over a temperate deciduous forest. *Atmos. Environ.* **45**, 2663–2674 (2011).
41. Xiao, H. W. et al.  $\delta^{15}\text{N}-\text{NH}_4^+$  variations of rainwater: application of the Rayleigh model. *Atmos. Res.* **157**, 49–55 (2015).
42. González, C. M. & Aristizábal, B. H. Acid rain and particulate matter dynamics in a mid-sized Andean city: The effect of rain intensity on ion scavenging. *Atmos. Environ.* **60**, 164–171 (2012).
43. Pan, Y. P. et al. Wet deposition and scavenging ratio of air pollutants during an extreme rainstorm in the North China Plain. *Atmos. Ocean. Sci. Lett.* **10**, 348–353 (2017).
44. Andronache, C. Estimates of sulfate aerosol wet scavenging coefficient for locations in the Eastern United States. *Atmos. Environ.* **38**, 795–804 (2004).
45. Huo, M. et al. Chemical character of precipitation and related particles and trace gases in the North and South of China. *J. Atmos. Chem.* **67**, 29–43 (2010).
46. Jylhä, K. Relationship between the scavenging coefficient for pollutants in precipitation and the radar reflectivity factor. Part I: derivation. *J. Appl. Meteorol.* **38**, 1421–1434 (1999).
47. van der Does, M., Korte, L. F., Munday, C. I., Brummer, G. A. & Stuur, J. B. W. Particle size traces modern Saharan dust transport and deposition across the equatorial North Atlantic. *Atmos. Chem. Phys.* **16**, 13697–13710 (2016).
48. Xu, D. et al. Multi-method determination of the below-cloud wet scavenging coefficients of aerosols in Beijing, China. *Atmos. Chem. Phys.* **19**, 15569–15581 (2019).
49. Zhang, L., Michelangeli, D. V. & Taylor, P. A. Numerical studies of aerosol scavenging by low-level, warm stratiform clouds and precipitation. *Atmos. Environ.* **38**, 4653–4665 (2004).
50. Wang, Y. et al. Disproportionate control on aerosol burden by light rain. *Nat. Geosci.* **14**, 72–76 (2021).
51. İlker, O. R. U. C., Akkoyunlu, B. O., Dogruel, M. & Tayanc, M. Chemical analysis of wet deposition sequential samples at Istanbul, Turkey. *Int. J. Eng. Res.* **10**, 126–132 (2018).
52. Lehmann, C. M., Bowersox, V. C. & Larson, S. M. Spatial and temporal trends of precipitation chemistry in the United States, 1985–2002. *Environ. Pollut.* **135**, 347–361 (2021).
53. Zhao, Y. et al. Atmospheric nitrogen deposition to China: a model analysis on nitrogen budget and critical load exceedance. *Atmos. Environ.* **153**, 32–40 (2017).
54. Liu, M. et al. Ammonia emission control in China would mitigate haze pollution and nitrogen deposition, but worsen acid rain. *Proc. Natl Acad. Sci. USA* **116**, 7760–7765 (2019).
55. Dennis, R. L., Mathur, R., Pleim, J. E. & Walker, J. T. Fate of ammonia emissions at the local to regional scale as simulated by the Community Multiscale Air Quality model. *Atmos. Pollut. Res.* **1**, 207–214 (2010).
56. Garrido, J. L., González-Rouco, J. F., Vivanco, M. G. & Navarro, J. Regional surface temperature simulations over the Iberian Peninsula: Evaluation and climate projections. *Clim. Dynam.* **55**, 3445–3468 (2020).
57. Sheppard, L. J. et al. Stress responses of *Calluna vulgaris* to reduced and oxidised N applied under ‘real world conditions’. *Environ. Pollut.* **154**, 404–413 (2008).
58. Lamarque, J. F. et al. Global and regional evolution of short-lived radiatively-active gases and aerosols in the Representative Concentration Pathways. *Clim. Change* **109**, 191–212 (2011).
59. Yu, F., Nair, A. A. & Luo, G. Long-term trend of gaseous ammonia over the United States: modeling and comparison with observations. *J. Geophys. Res.* **123**, 8315–8325 (2018).
60. Pinder, R. W., Adams, P. J. & Pandis, S. N. Ammonia emission controls as a cost-effective strategy for reducing atmospheric particulate matter in the eastern United States. *Environ. Sci. Technol.* **41**, 380–386 (2007). 2.
61. Guo, Y. X. et al. Air quality, nitrogen use efficiency and food security in China are improved by cost-effective agricultural nitrogen management. *Nat. Food* **1**, 648–658 (2020).
62. Trebs, I. et al. Dry and wet deposition of inorganic nitrogen compounds to a tropical pasture site (Rondônia, Brazil). *Atmos. Chem. Phys.* **6**, 447–469 (2006).
63. Pleim, J. & Ran, L. Surface flux modeling for air quality applications. *Atmosphere* **2**, 271–302 (2011).
64. Schoof, J. T. & Robeson, S. M. Projecting changes in regional temperature and precipitation extremes in the United States. *Weather Clim. Extremes* **11**, 28–40 (2016).
65. Zhang, L. et al. Agricultural ammonia emissions in China: reconciling bottom-up and top-down estimates. *Atmos. Chem. Phys.* **18**, 339–355 (2018).
66. Leneman, H., Oudendag, D. A., Van der Hoek, K. W. & Janssen, P. H. M. Focus on emission factors: a sensitivity analysis of ammonia emission modelling in the Netherlands. *Environ. Pollut.* **102**, 205–210 (1998).
67. Xu, R. et al. Global ammonia emissions from synthetic nitrogen fertilizer applications in agricultural systems: empirical and process-based estimates and uncertainty. *Glob. Chang Biol.* **25**, 314–326 (2009).
68. Fowler, D. et al. Atmospheric composition change: ecosystems–atmosphere interactions. *Atmos. Environ.* **43**, 5193–5267 (2009).
69. Flechard, C. R. et al. Advances in understanding, models and parameterizations of biosphere–atmosphere ammonia exchange. *Biogeosciences* **10**, 5183–5225 (2013).
70. Flechard, C. R., Fowler, D., Sutton, M. A. & Cape, J. N. A dynamic chemical model of bi-directional ammonia exchange between semi-natural vegetation and the atmosphere. *Q. J. R. Meteorol. Soc.* **125**, 2611–2641 (1999).
71. Nemitz, E., Milford, C. & Sutton, M. A. A two-layer canopy compensation point model for describing bi-directional biosphere–atmosphere exchange of ammonia. *Q. J. Roy. Meteorol. Soc.* **127**, 815–833 (2001).
72. Wen, Z. et al. Changes of nitrogen deposition in China during 1980 and 2018. *Environ. Int.* **144**, 106022 (2020).
73. Sorteberg, A. & Hov, Ø. Two parametrizations of the dry deposition exchange for  $\text{SO}_2$  and  $\text{NH}_3$  in a numerical model. *Atmos. Environ.* **30**, 1823–1840 (1996).
74. Han, X., Zhang, M., Skorokhod, A. & Kou, X. X. Modeling dry deposition of reactive nitrogen in China with RAMS-CMAQ. *Atmos. Environ.* **166**, 47–61 (2017).
75. Dennis, R. L. et al. Sensitivity of continental United States atmospheric budgets of oxidized and reduced nitrogen to dry deposition parameterizations. *Philos. Trans. R. Soc. B* **368**, 20130124 (2013).
76. Pleim, J. E., Bash, J. O., Walker, J. T. & Cooter, E. J. Development and evaluation of an ammonia bidirectional flux parameterization for air quality models. *J. Geophys. Res.* **118**, 3794–3806 (2013).
77. Sutton, M. A. et al. Towards a climate-dependent paradigm of ammonia emission and deposition. *Philos. Trans. R. Soc. B* **368**, 20130166 (2013).
78. Zhang, L., Wright, L. P. & Asman, W. A. H. Bi-directional air-surface exchange of atmospheric ammonia: a review of measurements and a development of a big-leaf model for applications in regional-scale air-quality models. *J. Geophys. Res.* **115**, D20310 (2010).
79. Liu, X., Xu, W., Du, E. Z., Pan, Y. P. & Goulding, K. Reduced nitrogen dominated nitrogen deposition in the United States, but its contribution to nitrogen deposition in China decreased. *Proc. Natl Acad. Sci. USA* **113**, E3590–E3591 (2016).
80. Du, E., de Vries, W., Galloway, J. N., Hu, X. Y. & Fang, J. Y. Changes in wet nitrogen deposition in the United States between 1985 and 2012. *Environ. Res. Lett.* **9**, 095004 (2014).
81. Wesely, M. L. Parameterization of surface resistances to gaseous dry deposition in regional-scale numerical models. *Atmos. Environ.* **23**, 1293–1304 (1989).
82. Zhang, L., Gong, S., Padro, J. & Barrie, L. A size-segregated particle dry deposition scheme for an atmospheric aerosol module. *Atmos. Environ.* **35**, 549–560 (2001).
83. Su, H. et al. Numerical simulation for dry deposition of ammonia and nitrogen dioxide in a small watershed in Jurong County of Jiangsu Province. *Chin. J. Agrometeorol.* **30**, 335–342 (2009). (in Chinese).
84. Zhang, L., Brook, J. R. A. & Vet, R. A revised parameterization for gaseous dry deposition in air-quality models. *Atmos. Chem. Phys.* **3**, 2067–2082 (2003).
85. Zhang, Y., Wang, T. J., Hu, Z. Y. & Xu, C. K. Temporal variety and spatial distribution of dry deposition velocities of typical air pollutants over different landuse types. *Clim. Environ. Res.* **9**, 591–604 (2004).
86. Zhang, G., Zhang, J. & Liu, S. M. Characterization of nutrients in the atmospheric wet and dry deposition observed at the two monitoring sites over Yellow Sea and East China Sea. *J. Atmos. Chem.* **57**, 41–57 (2007).
87. Zhang, L. et al. Dry deposition of individual nitrogen species at eight Canadian rural sites. *J. Geophys. Res.* **114**, D02301 (2009).
88. Zhang, Y., Yu, Q., Ma, W. C. & Chen, L. M. Atmospheric deposition of inorganic nitrogen to the eastern China seas and its implications to marine biogeochemistry. *J. Geophys. Res.* **115**, D00K10 (2010).
89. Schiferl, L. D. et al. Interannual variability of ammonia concentrations over the United States: Sources and implications. *Atmos. Chem. Phys.* **16**, 12305–12328 (2016).

## ACKNOWLEDGEMENTS

This study was supported by the National Natural Science Foundation of China (42121004, 42230701, 41905086, 41905107, 42077205, and 41425020), the second Tibetan Plateau Scientific Expedition and Research Program (2019QZKK0604), the Special Fund Project for Science and Technology Innovation Strategy of Guangdong Province (2019B121205004), the AirQuip (High-resolution Air Quality Information for Policy) Project funded by the Research Council of Norway, the Collaborative

Innovation Center of Climate Change, Jiangsu Province, China, and the high-performance computing platform of Jinan University. The authors thank Dr. Huan Liu (Tsinghua University), Dr. Lin Zhang (Peking University), Dr. Sayantan Sarka (Indian Institute of Technology), and Dr. Padmaja Krishnan (National University of Singapore) for valuable suggestions and improvements to the paper. The authors would like to thank the four anonymous reviewers for their constructive feedback.

## AUTHOR CONTRIBUTIONS

W.H.C., S.G.J., X.M.W., and M.S. conceived the study and led the analysis. W.H.L. helped with precipitation data processing. B.Q.Z., W.W.W., and J.Y.M. helped with emissions and ammonium deposition data processing. M.C. helped with the EMEP model simulation. C.F., A.G., P.F.Y., X.J.L., G.R.Y., and G.C. provided important views on the study. All co-authors contributed to improving the analysis and interpretation.

## COMPETING INTERESTS

The authors declare no competing interests as defined by Nature Research, or other interests that might be perceived to influence the interpretation of the article.

## ADDITIONAL INFORMATION

**Supplementary information** The online version contains supplementary material available at <https://doi.org/10.1038/s41612-023-00390-7>.

**Correspondence** and requests for materials should be addressed to Xuemei Wang or Min Shao.

**Reprints and permission information** is available at <http://www.nature.com/reprints>

**Publisher's note** Springer Nature remains neutral with regard to jurisdictional claims in published maps and institutional affiliations.



**Open Access** This article is licensed under a Creative Commons Attribution 4.0 International License, which permits use, sharing, adaptation, distribution and reproduction in any medium or format, as long as you give appropriate credit to the original author(s) and the source, provide a link to the Creative Commons license, and indicate if changes were made. The images or other third party material in this article are included in the article's Creative Commons license, unless indicated otherwise in a credit line to the material. If material is not included in the article's Creative Commons license and your intended use is not permitted by statutory regulation or exceeds the permitted use, you will need to obtain permission directly from the copyright holder. To view a copy of this license, visit <http://creativecommons.org/licenses/by/4.0/>.

© The Author(s) 2023